

# A low-temperature partial-oxidation-methanol micro reformer with high fuel conversion rate and hydrogen production yield

Hsueh-Sheng Wang <sup>a</sup>, Kuo-Yang Huang <sup>a</sup>, Yuh-Jeen Huang <sup>b,\*</sup>, Yu-Chuan Su <sup>a</sup>, Fan-Gang Tseng <sup>a,\*</sup>

<sup>a</sup> Department of Engineering and System Science, National Tsing Hua University, Hsinchu, Taiwan

<sup>b</sup> Department of Biomedical Engineering and Environmental Sciences, National Tsing Hua University, Hsinchu, Taiwan



## HIGHLIGHTS

- A low-operating temperature of the POM-mode micro methanol reformer is obtained.
- The effect of channel design on the performance is studied.
- The effect of solid content and binder' ratio on the performance is studied.
- The centrifugal process is benefit for the modification of performance.
- 98% of methanol conversion rate of the micro reformer can be obtained at 180 °C.

## ARTICLE INFO

### Article history:

Received 29 April 2014

Received in revised form 14 August 2014

Accepted 7 October 2014

Available online 7 November 2014

### Keywords:

Hydrogen production

Centrifugal catalyst coating

Micro POM methanol reformer

Micro fluidics

Low temperature reforming

## ABSTRACT

A partial oxidation methanol micro reformer (POM- $\mu$ Reformer) with finger-shaped channels for low operating temperature and high conversing efficiency is proposed in this study. The micro reformer employs POM reaction for low temperature operation (less than 200 °C), exothermic reaction, and quick start-up, as well as air feeding capability; and the finger type reaction chambers for increasing catalyst loading as well as reaction area for performance enhancement. In this study, centrifugal technique was introduced to assist on the catalyst loading with high amount and uniform distribution. The solid content (S), binder's ratio (B), and channel design (the ratio between channel's length and width, R) were investigated in detail to optimize the design parameters. Scanning electron microscopy (SEM), gas chromatography (GC), and inductively coupled plasma-mass spectrometer (ICP-MS) were employed to analyze the performance of the POM- $\mu$ Reformer. The result depicted that the catalyst content and reactive area could be much improved at the optimized condition, and the conversion rate and hydrogen selectivity approached 97.9% and 97.4%, respectively, at a very low operating temperature of 180 °C with scarce or no binder in catalyst. The POM- $\mu$ Reformer can supply hydrogen to fuel cells by generating 2.23 J/min for 80% H<sub>2</sub> utilization and 60% fuel cell efficiency at 2 ml/min of supplied reactant gas, including methanol, oxygen and argon at a mixing ratio of 12.2%, 6.1% and 81.7%, respectively.

© 2014 Elsevier Ltd. All rights reserved.

## 1. Introduction

Fuel cells have emerged as alternative power sources potentially for various applications in transportation, portable electronics, and residential power sources owing to their high overall system efficiencies, high energy density, and eco-friendly nature. Among various applicable areas, portable devices are one of the promising areas for fuel cell applications, especially for small proton-exchange membrane fuel cells (PEMFC), due to its high efficiency and high volumetric energy densities (up to 2500 Wh l<sup>-1</sup> for

hydrogen or 5000 Wh l<sup>-1</sup> for liquid methanol, when compared to 400 Wh l<sup>-1</sup> provided by lithium-ion batteries) [1,2]. However, the major issue encountered in PEMFC is the need of fuel supply from pure hydrogen based sources. Therefore, by reforming hydrogen-rich hydrocarbon fuels, such as methanol, ethanol or acetic acid, has been becoming a more practical way for real applications.

Currently, methanol has become a more favored source for hydrogen production owing to its sulfur-free, high hydrogen-to-carbon ratio, low vaporization temperature, low reaction temperature, and high energy density, when compared to other hydrocarbon fuels. In many studies, oxidation of methanol can offer an easy way to transform methanol into the hydrogen-rich gas via either decomposition of methanol (DM), steam reforming methanol reaction (SRM), or partially oxidative methanol

\* Corresponding authors.

E-mail addresses: [yjhuan@mx.nthu.edu.tw](mailto:yjhuan@mx.nthu.edu.tw) (Y.-J. Huang), [fangang@ess.nthu.edu.tw](mailto:fangang@ess.nthu.edu.tw) (F.-G. Tseng).

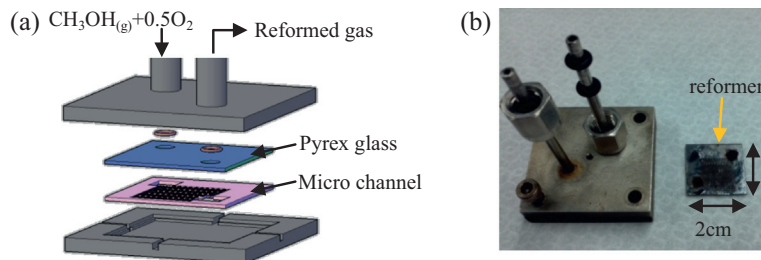


**Fig. 1.** The micro reactor design. (a) Schematic of reactor design and (b) picture of reactor utilized in this study.

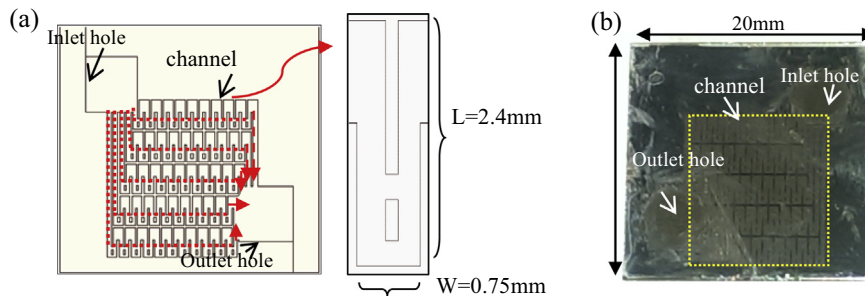
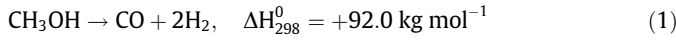


**Fig. 2.** (a) The detail channel design of varied micro reformer, and  $R = W/L$ ; (b) the fabricated micro reformer with coated channel.

reforming reaction (POM). The equations of these three reactions are as followed (Eq. (1)–(3)) [3–5]:



So far, the steam reforming reaction (Eq. (2)) was generally considered as the major way for hydrogen production for its high hydrogen yield (for one mole methanol generating 3 mol hydrogen). However, the reaction is not only endothermic requiring external heat input; but also produces a considerable amount of CO (>100 ppm) which poisons Pt catalyst in the PEMFC to deteriorate fuel cell performance. As a result, SRM reactor is often equipped with an external heating system and CO remover (by water-gas-shift reaction (WGSR) for CO oxidation), which greatly increases the cost and extra space for system integration accordingly [6,7].

An alternative way to produce hydrogen with relatively lower amount of CO is by using POM reaction. Even though its hydrogen production rate is about 33% lower than that of SRM method, it provides some advantages such as rather low operating temperature (250 °C, compared to 350 °C for SRM), exothermic reaction without the need of extra heating, quick start-up, and only requiring air instead of steam for reaction [8]. Therefore, POM reaction is employed in this study.

To reduce the working temperature without dramatically dropped performance for directly integration with portable PEMFC, the design of the microfluidic channels and the characteristics of deposited catalyst in the reaction chamber are very important [9–11]. Recently, many researches focused on how to improve the performance of micro reformer by investigating various parameters, such as operation temperature, fuel feeding rate, micro channel designs, internal pressure drop, and content as well as quality of the coated catalyst in the reformer [12]. According to Eqs. (1) and (3), it is obvious that the operating temperature and pressure play an opposite roles on the rate of H<sub>2</sub> production. Even though the conversion rate of methanol increases with the temperature, however the raise of pressure and temperature will not only

deteriorate the yield of hydrogen but also expedite the output of carbon monoxide [13,14], which will poison the Pt contained in the PEMFC [15]. Hence, Hsieh et al. [16] depicted that by combining interdigitated and mesh type of channels together the pressure drop of the reformer can be lowered down, thus enhancing reformer performance. Moreover, some reports [16,17] also indicated that high reaction surface area, well coated catalyst, and low pressure drop of the fluidic channels, were the three keys to keep reformer in high performance. These conditions can be achieved by introducing catalyst slurry with fill-and-dry coating process to form a catalyst layer with porous and relatively fine structure on the channel's wall [18,19]. On the other hand, there were also studies focusing on the integration of micro channel by MEMS technology [20] and the methods for catalyst preparation and surface coating [21,22], however the effective operating temperature of the micro reformers when keeping a high conversion rate of methanol (>85%) are still high (>250 °C) for direct PEMFC (usually operated in 60–80 °C) integration.

**Table 1**  
The chemical notations of metallic precursors.

Manufacturer	The type of precursors		
	Mn(NO <sub>3</sub> ) <sub>2</sub> ·4H <sub>2</sub> O Merk KGaA (Germany)	Cu(NO <sub>3</sub> ) <sub>2</sub> ·3H <sub>2</sub> O Sigma-Aldrich (USA)	Zn(NO <sub>3</sub> ) <sub>2</sub> ·6H <sub>2</sub> O Sigma Aldrich (USA)
Assay (%)	≥98.5 Impurities ≤ (mg/kg)	≥98	≥99
Cl <sup>-</sup>	10	50	50
SO <sub>4</sub> <sup>2-</sup>	50	50	100
Ca	10	50	50
Fe	5	50	50
K	50	100	100
Na	50	100	100
Ni	5	50	50
Pb	10	50	50
Zn	10	50	50
Cu	5	50	50

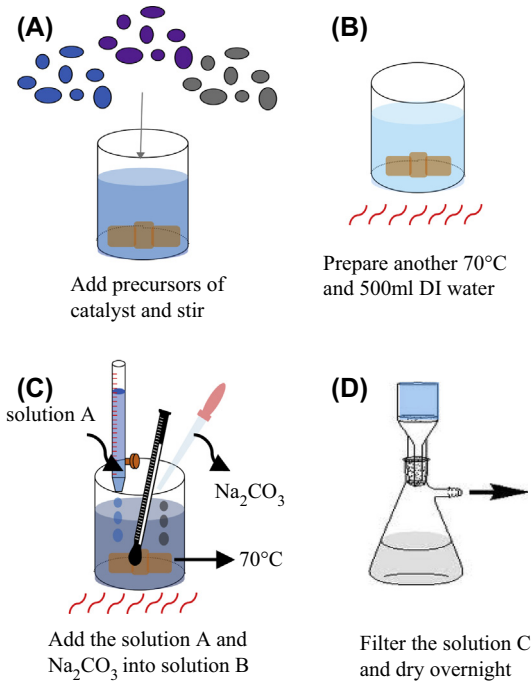


**Fig. 3.** The fabrication process of catalyst.

Therefore, this study introduces a novel design of micro-POM-Reformer to further lower down the operation temperature to 180 °C with a high performance for hydrogen conversion rate and selectivity approaching 97.9% and 97.4%, respectively.

## 2. Experimental

### 2.1. Design of micro methanol POM reformer

**Fig. 1a** shows a schematic of the integrated micro POM-reformer composed of one silicon-based micro channel and one cover plate with inlet/outlet holes. **Fig. 1b** is the interior design and optical image of a fully integrated reformer used in this study. The detailed design of each component is depicted in **Fig. 2**. The micro channel is made by photolithography process on silicon substrate and consists of a volume of 20 mm \* 20 mm \* 500  $\mu\text{m}$ . On the top view of this plate, finger-shaped rectangular channels incorporated with azimuthal interconnection routes are employed as catalyst container and methanol reformer. The flow path way inside is described as the red dash line of **Fig. 2(a)**. The effect of  $R$  value ( $R = L/W$ ) on the performance is investigated via fixing the  $W$  value and adjusting  $L$  value, and their definitions are shown in **Fig. 2a**. The channel has a width of 750  $\mu\text{m}$  on average and depth of 350  $\mu\text{m}$ . **Fig. 2b** shows a completed micro POM reformer with a cover plate area of 20 mm \* 20 mm \* 700  $\mu\text{m}$  after fully catalyst loading. In testing, methanol steam-oxygen-argon mixture is injected into the micro methanol reformer from the inlet port and the produced gases are released from the outlet port.

### 2.2. Fabrication of catalyst

Catalysts with designed compositions of Cu–Mn–Zn, which the chemical notations of metallic precursors is shown on **Table 1**, were prepared via the method by deposition precipitation and co-precipitation (CP) [23–25], as shown in **Fig. 3**. The 100 ml of mixture of copper (II) nitrate trihydrate ( $\text{Cu}(\text{NO}_3)_2 \cdot 3\text{H}_2\text{O}$ ), manganese (II) nitrate tetrahydrate ( $\text{Mn}(\text{NO}_3)_2 \cdot 4\text{H}_2\text{O}$ ), and zinc nitrate hexahydrate ( $\text{Zn}(\text{NO}_3)_2 \cdot 6\text{H}_2\text{O}$ ) precursor solutions in the ratio of

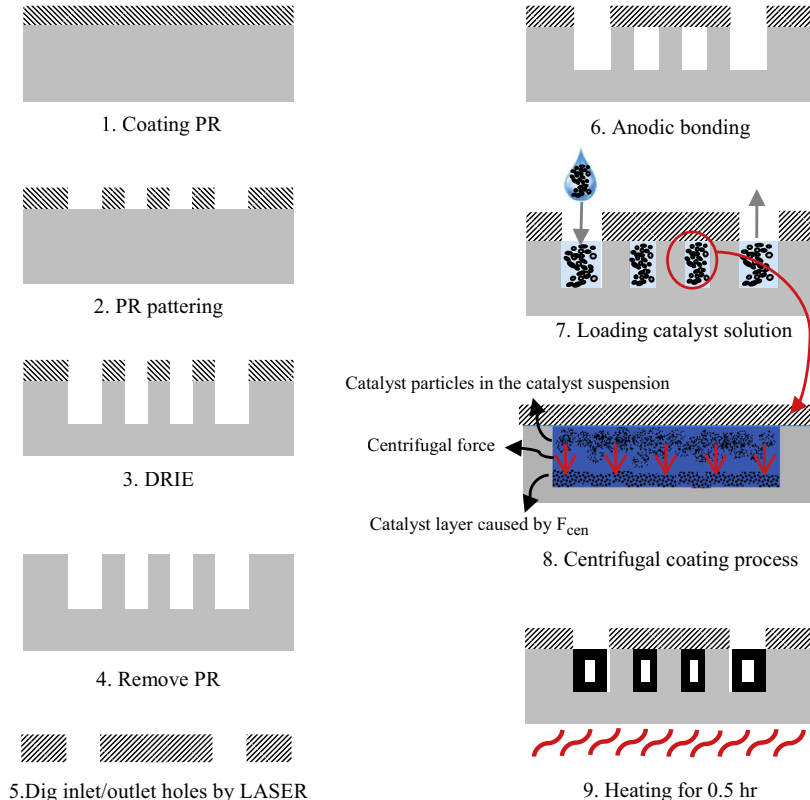


**Fig. 4.** The fabrication process of the micro reformer.

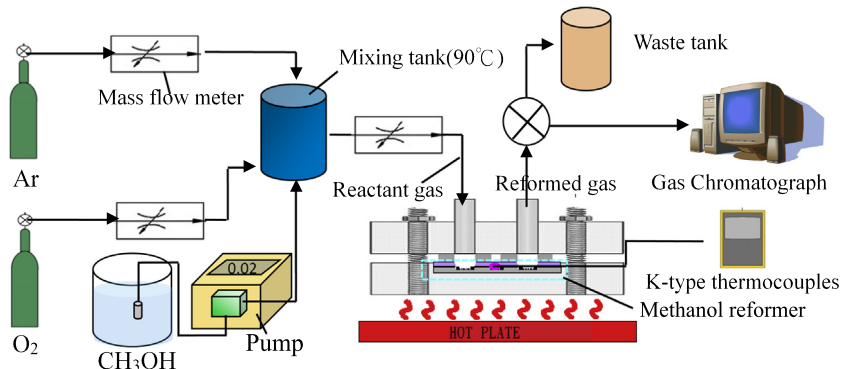


Fig. 5. The experimental setup.

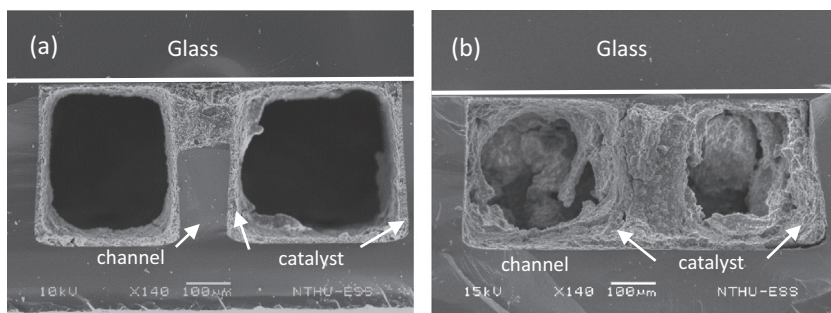


Fig. 6. The top-view SEM image of catalyst layer via different coating methods. (a) Conventional fill-and-dry coating method and (b) the centrifugal coating method.

30 wt.% of Cu, 20 wt.% of Mn and 50 wt.% of Zn or the 0.24 M of copper nitrate salt, the 0.18 M of manganese nitrate salt and the 0.38 M of zinc nitrate salt stored in burette were dropped into 500 ml of deionized water at 70 °C under stirring condition. At the meantime, 2 M of Na<sub>2</sub>CO<sub>3</sub> was added to maintain the mixture at pH 7 while the solution A was dropped into 500 ml of DI water and to start the crystallization of catalyst during titration process till the precursor solution is completely used up. Afterwards, the solution of the mixture was kept to be under stirring condition to carry out aging process to form appropriate crystal structure. At the same time, the solution is getting basic by the reason of the release of hydrogen carbonate ion ( $-HCO_3^-$ ). After the pH value

of catalyst solution reaches pH 8 during the aging process, the insolubly metallic-compound Cu–Mn–Zn precipitates, including copper carbonate, copper dihydroxide, manganese carbonate and zinc oxide etc., were filtrated and washed fully with deionized water, and then dried at 105 °C for overnight. The preparation of catalyst was completed after calcination in air at 400 °C for 2 h.

### 2.3. Fabrication of micro reformer

Fig. 4 shows the fabrication steps of the micro methanol reformer. The micro channels with finger-shaped grooves were first fabricated on silicon (100) wafer by photolithography and deep

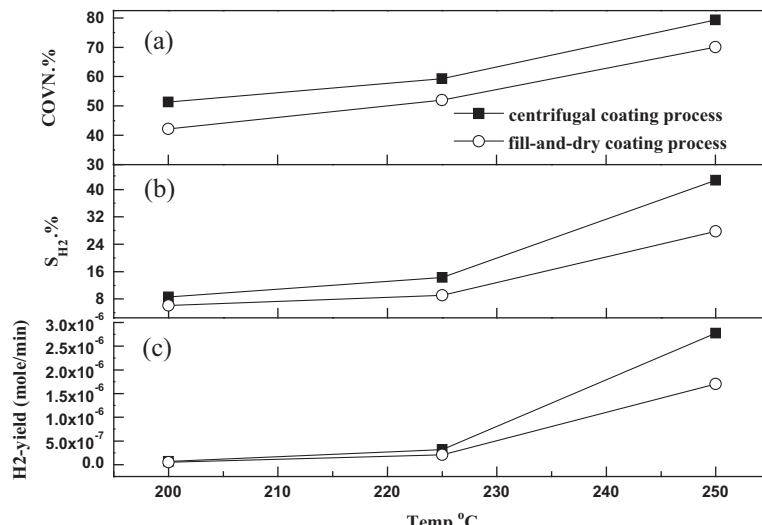


Fig. 7. The GC analysis of the effect on performance of different catalytic coating processes. (a) The methanol conversion rate of micro reformer; (b) the hydrogen selectivity of micro reformer and (c) the hydrogen yield of micro reformer.

silicon reactive ion etching (DRIE) process. Then, groove-walls were treated by oxygen plasma for hydrophilic property. Pyrex glasses with inlet/outlet holes machined by laser dripping process were anodic bonded on the chips to obtain micro-channels. The catalytic suspension was then prepared before loaded into the micro reformer. Different catalytic suspensions with various ratios of solid contents ( $S = (X + Y)/(X + Y + Z)$ ) and binders ( $B = Y/(X + Y)$ ) were tested for performance comparison. Where  $X$ ,  $Y$  and  $Z$  are the weights (mg) of catalyst, AlOOH-based binder, and water, respectively.

After micro reformer was loaded with catalytic solution through fill-and-dry process, in order to create a dendrite-like coating layer to increase the active area, centrifugal process (patent APPL. NO: 13585519) was introduced to force the catalyst particle of the suspension to deposit from the bottom to the top of channel, and then the chip with catalyst was dried at 105 °C for 30 min. This centrifugal process can avoid the block of channel and get more uniform catalyst layer. Finally, the micro reformer fabrication was completed after repeating the coating process ten times followed by annealing at 400 °C for 2 h.

#### 2.4. Micro POM-reformer testing

The experimental setup for the micro POM reformer performance test is shown Fig. 5. The main test apparatus is composed of the reactant supply system, integrated POM reformer, a hotplate to control the operating temperature, data acquisition system with GC unit for product analysis, and K-type thermocouples for temperature measurement. For the reactant supply system, argon was employed as the carrier gas, oxygen and liquid methanol were used as the reactant/fuel, and the feed rate were set as 81.7 and 6.1 ml/min through the mass flow controller (Brooks instrument, 5850E), and 0.02 ml/min via peristaltic pump (YSMC, Taiwan, ROC) to obtain the steam flow rate of 12.2 ml/min after evaporating, respectively. The composition of the reactant gas followed the stoichiometric of the POM reaction. The reactant gas were plenary premixed and preheated in the mixing chamber to 90 °C before delivered into the micro-methanol reformer at designated feed rate, 2 ml/min, to carry out the reforming reaction. The reformed gas stream passed through a valve to feed into GC analyzer for analyzing H<sub>2</sub>, CO, CO<sub>2</sub>, and the remained MeOH compositions. The methanol conversion rate, hydrogen yield rate,

**Table 2**

The ICP-MS measurement of the catalyst amount for reformers of different  $R$  ratios.

$R$	Cu	Mn	Zn	<sup>a</sup> $M_{Cu+Mn+Zn}$ (mg)
	<sup>b</sup> wt.%			
2.9	31.1	18.7	50.2	3.8
3.4	31.1	18.7	50.2	5.1
4.3	31.4	19.7	48.9	2.9
4.7	30.8	19.7	49.5	2.7

<sup>a</sup>  $M_{Cu+Mn+Zn}$ (mg): the sum of the mass of metals contained in the catalyst.

<sup>b</sup> wt.%: the mass percentage of metals contained in the catalyst.

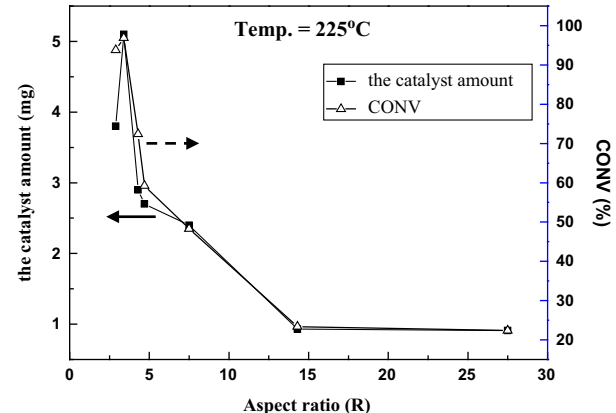


**Fig. 9.** The relationship between the catalyst amount, the aspect ratio ( $R$ ) and the conversion rate.

and hydrogen selectivity were obtained based on the measured compositions in the reformed gases.

### 3. Results and discussion

#### 3.1. Influence of centrifugal process

Compared to micro packed bed with catalyst fully packed inside the chamber, the micro-channel reformer with catalyst only coated on channel surface has some advantages including no or minor hotspot problem, much smaller pressure drop, and good

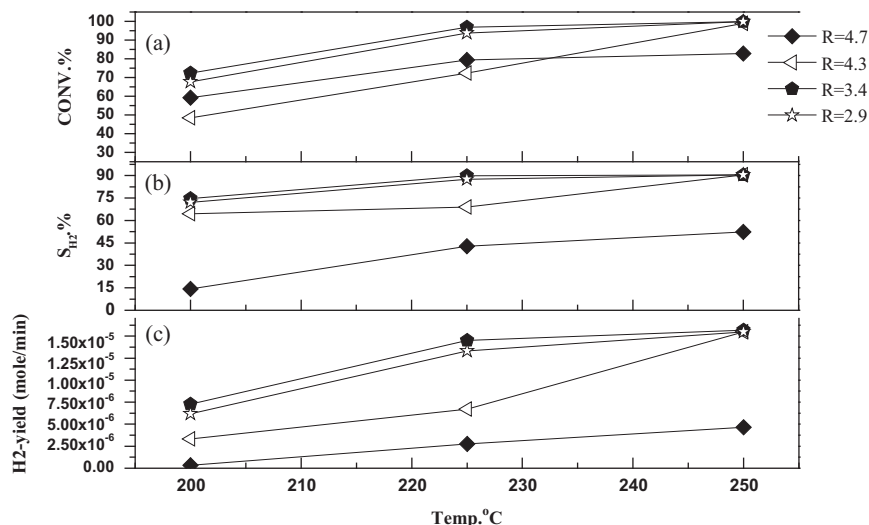


**Fig. 8.** the GC analysis results for reformers of different channel aspect ratio,  $R$ . (a) The methanol conversion rate of micro reformer; (b) the hydrogen selectivity of micro reformer and (c) the hydrogen yield of micro reformer.

**Table 3**

The ICP-MS measurement of the catalyst amount for reformers of different binder's ratio ( $B$ ).

$B$	Cu	Mn	Zn	<sup>a</sup> $M_{Cu+Mn+Zn}$ (mg)
	<sup>b</sup> wt.%			
60	30.6	18.9	50.5	2.7
35	30.1	18.8	50.1	8.2
10	31.1	18.7	50.2	15.7
0	30.1	19	50.9	17.4

<sup>a</sup>  $M_{Cu+Mn+Zn}$ (mg): the sum of the mass of metals contained in the catalyst.

<sup>b</sup> wt.%: the mass percentage of metals contained in the catalyst.

distribution of catalyst across the micro channel. However, the efficiency is still relatively lower than that in micro-packed bed since the addition of sol of alumina-based binder to the catalyst leads to the reduction of the effective surface area exposed to reactants, whereas the effective surface area exposed to reactants is unchanged for the micro-packed reactor [26]. For further enhancing the performance of the micro-reformer, especially in lower temperature operation range, it is essential to increase the amount, thickness, and roughness of the coated catalyst in the reformer to simulate the catalyst packing structures in pack-bed condition. Therefore, we introduced centrifugal force during the process of coating catalyst in the finger type micro channel to increase the roughness and loading of the catalyst layer, as shown in Fig. 6. Compared the difference of SEM images between Fig. 6a and b, the thickness and roughness of catalyst layer via the centrifugal coating method are much more than those by conventional fill-and-dry coating methods. In this study, several parameters were

compared to characterize the performance of each micro reformer, including methanol conversion rate (CONV.%), hydrogen selection rate ( $S_{H2} \cdot \%$ ), and hydrogen production yield ( $H_2$ -yield).

They are defined as:

$$\text{CONV.}\% = \frac{m2}{m1} \times 100\% \quad S_{H2} \cdot \% = \frac{m3}{m3 + m4} \times 100\%$$

where  $m_{1-4}$  is the mole per minute of the methanol fed into micro reformer, the consumed methanol, the produced hydrogen, and water, respectively. From the GC-analysis result, as shown in Fig. 7, we learned that the micro reformer with centrifugal coated catalyst did have about 10–20% higher performance in the entire testing temperature range, owing to the better thickness control and much rougher surface of catalyst inside reformer to increase reactive area.

### 3.2. Influence of channel aspect ratio ( $R$ ), solid content ( $S$ ), and binder's ratio ( $B$ ) on reformer performance

In order to further improve the performance of micro reformer, we individually investigate several important parameters including channel aspect ratio, binder's ratio, as well as solid contents, and then an optimized combination of those parameters will be considered to carry out a high efficient micro reformer.

#### 3.2.1. Channel aspect ratio ( $R$ )

The finger-shaped micro channel, fabricated for containing catalyst, consists of oblong-shaped columns with interconnected side passages, (as shown in Fig. 2a) for not only providing multiple pathways for gas transportation into the very bottom of the

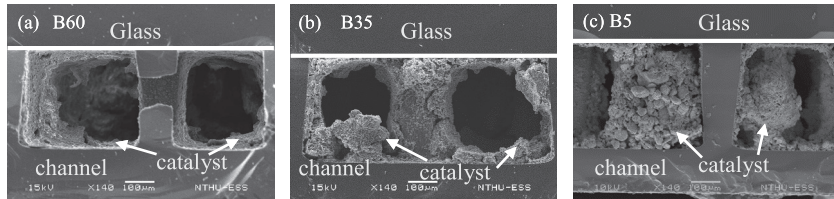


**Fig. 10.** 140X SEM images of catalyst layers in the micro reformers with different binder's ratio,  $B$ . The cross section view of the channel in the micro reformer with (a)  $B = 60$ , (b)  $B = 35$ , and (c)  $B = 5$ .

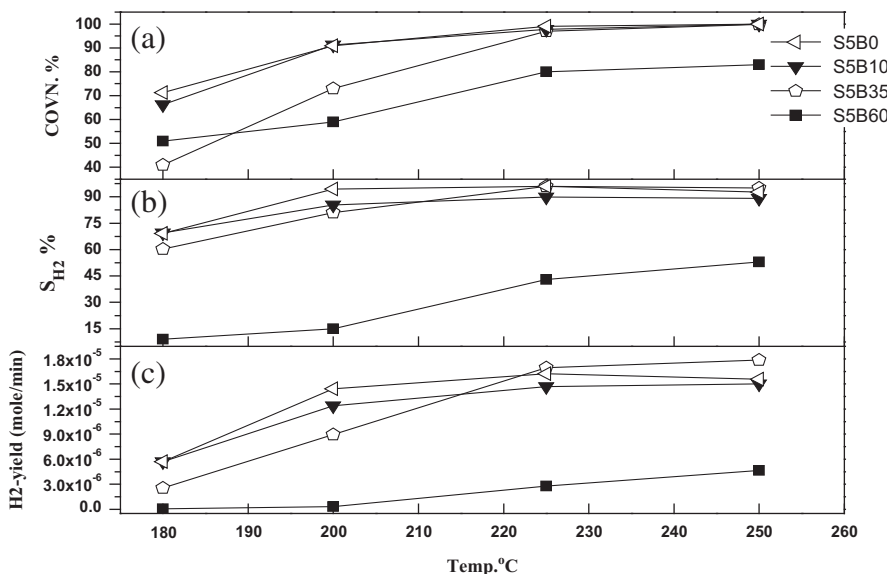


**Fig. 11.** GC analysis results for reformers of different binder's ratio,  $B$ . (a) Methanol conversion rate, (b) hydrogen selectivity, and (c) hydrogen yield.

**Table 4**

The BET surface area and porosity of different combination of catalysts.

Parameter	Porosity (%)	BET ( $\text{m}^2/\text{g}$ )
Pure catalyst (B0)	35.69	55
S5B10	31.85	54.5
S5B35	48.32	81
S5B60	51.1	102.9
Pure binder (B100)		180

channel but also allowing the reduction of pressure drop for promoting reforming reaction. The value of  $R$  is an important parameter to define the outmost reachable region for reforming process, as shown in Fig. 2(a). For catalyst loading and each rectangular channel, large  $R$  will intuitively provide a larger area for catalyst accommodation while catalyst loading resistance and gas flow resistance will increase as well. On the other hand, lower  $R$  may not provide long enough pathways for catalyst accommodation and thus deteriorate the gas reforming efficiency. As a result, an optimized value of  $R$  is anticipated for the best performance of the reformer. Several different type  $R$ , ranging from 2.9 to 4.7, are selected for investigation. At the same time, more amounts of entrance of channel will be introduced while decreasing the  $R$  value in order to raise the space utility of the chip, and we found out that the performance of micro reformer increases with decreased  $R$  until  $R = 3.4$ , and then slightly decreases at  $R = 2.9$ . The CONV.%,  $S_{\text{H}_2}.$ % as well as hydrogen yield of the reformer at  $R = 3.4$  reached 91%, 90%, and  $1.45 \times 10^{-5}$  mole/min at 225 °C, respectively, as shown in Fig. 8. There are two reasons to explain the result. The first reason is that each rectangular channel with smaller  $R$  value might allow reactive gas to flow the very bottom of channel and reduce the pressure drop inside so that it will benefit the POM reaction; Secondly, the catalyst loading might decrease with decreased  $R$  due to the decrement of surface area of the single channel. Thus, we increase the total volume of channel to overcome this problem, and 0.0487  $\text{cm}^3$  of the largest volume in this study is obtained at  $R = 3.4$ . Not only the performance of micro reformer can be modified, but also the expected amount of catalyst contained in the micro reformer is increased until  $R$  value was reduced to 3.4 owing to the positive relationship between space time and total volume. From the ICP-MS measurement results, as tabulated in Table 2, the amount of

**Table 5**

The ICP-MS data of the catalyst amount of different solid content.

S	Cu	Mn	Zn	<sup>a</sup> $M_{\text{Cu}+\text{Mn}+\text{Zn}}$ (mg)
<sup>b</sup> wt.%				
5	30.1	18.7	51.2	13.8
10	30.4	20.1	49.5	14.2
15	31.1	19.6	49.3	15.1

<sup>a</sup>  $M_{\text{Cu}+\text{Mn}+\text{Zn}}$  (mg): the sum of the mass of metals contained in the catalyst.<sup>b</sup> wt.%: the mass percentage of metals contained in the catalyst.

catalyst contained in the micro reformer is gradually increased with the decreased  $R$  values until 3.4, and then slightly decreased at  $R = 2.9$ , which is in consistent with the reformer performance, as shown in Fig. 9. Therefore,  $R = 3.4$  is selected throughout the rest of experiments for micro reformer design.

### 3.2.2. Binder's ratio (B)

Recently, many researches mixed AlOOH-based binder with catalyst to enhance the adhesion between catalyst and Si-based channel via a fill-and-dry coating process [17]. However, AlOOH-based particle occupied significant spaces for blocking catalytic particle reacting in micro channels which greatly reduce the performance of micro reformer in spite of the enhancement of the adhesion. Thus, careful study of the binder amount is critical for high performance micro reformer. In this study, different ratios  $B$  in the catalyst solution ranged from 60 to 0 were tested. The solutions were injected into the micro-channels by a peristaltic pump, and then the solid contents of catalyst slurries were deposited on the micro-channel sidewalls by the centrifugal technique mentioned earlier. The catalyst slurries were dried out at 105 °C for 30 min inside the micro-channels. The catalyst coating process was repeated ten times by the aforementioned steps and finally annealed at 400 °C for 2 h. The weight ratio of binder to solid catalysts ( $B$ ) was varied for the study, as tabulated in Table 3. The catalyst content was increased from 2.7 to 17.4 mg while  $B$  was reduced from 60 to 0 with  $B = 0$ , indicating the highest occupation volume of the catalyst in the microchannels, as shown in the Fig. 10. Fig. 11 shows that the performance of micro-reformers with different binder ratios from 60 to 0. The highest performance occurred when  $B = 0$ , where the methanol conversion rate, hydrogen selectivity, and hydrogen yield of the micro-methanol

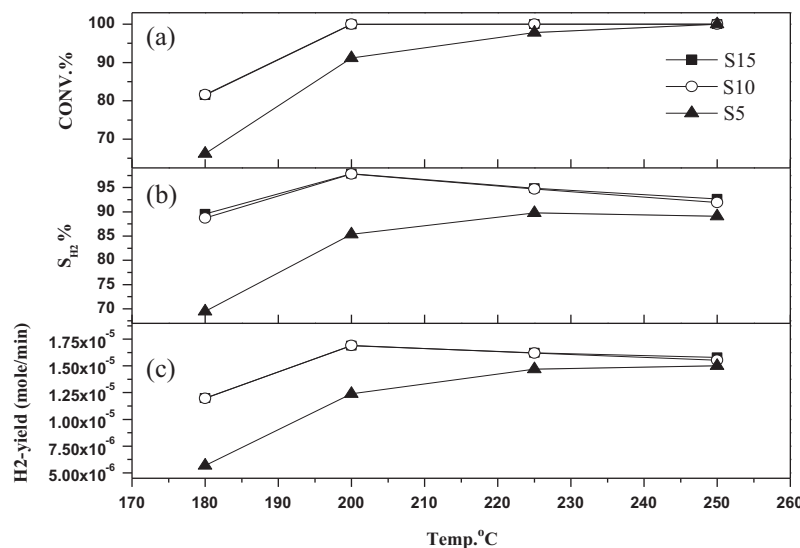
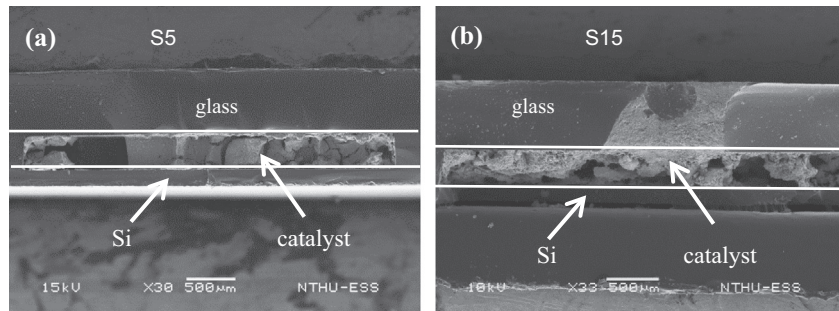


Fig. 12. GC analysis results for reformers of different solid contents,  $S$ . (a) The methanol conversion rate of micro reformer; (b) the hydrogen selectivity of micro reformer and (c) the hydrogen yield of micro reformer.



**Fig. 13.** The SEM images of catalyst layers in the micro reformers with different solid contents,  $S$ . (a) The side view of channels in the micro reformer with  $S = 5$  and (b) the side view of channels in the micro reformer with  $S = 15$ .

**Table 6**

The influence of various testing parameters on the performance at 180 °C.

Performance	Parameters		
	$R$ (200 °C) 27.5–2.9	$S$ 5–15	$B$ 60–0
CONV. %	22–72	66–82	45–72
$S_{H_2}$	12–75	70–90	9–70
$H_2$ -yield (mole/min)	$1.6 \times 10^{-8}$ to $7.3 \times 10^{-6}$	$5.7 \times 10^{-6}$ to $1.2 \times 10^{-5}$	$7.1 \times 10^{-8}$ to $5.7 \times 10^{-6}$

reformer approached 100%, 92%, and  $1.56 \times 10^{-5}$  mole min $^{-1}$  at 250 °C, respectively. For operating temperature between 200 and 250 °C, the performance of micro reformer still kept a steady and high performance when  $B = 0$ , indicating the importance of binder blockage issue to catalyst reaction. Especially, even if the operating temperature was lowered down to 180 °C, reasonable conversion rate of 71% and hydrogen selectivity of 70% were still observed. The hydrogen selectivity was also improved 6 times from 15% to 90% at 200 °C with  $B = 0$ . On the other hand, the addition of AlOOH-based binder though may not decrease the adhesion between the catalyst layer and channel wall, however, it may reduce the adhesion among catalysts and lead to a thin coating layer, which is not beneficial to the overall catalytic performance especially in low temperature range, as shown in Fig. 11. Besides, in the current micro channel design, the catalyst can be held partially by the branched finger type structures, thus large amount

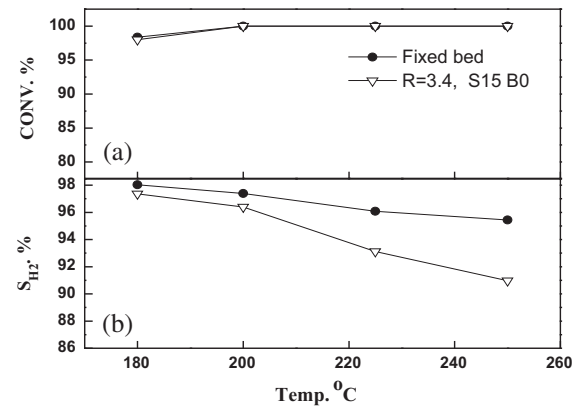


**Fig. 15.** GC analysis results of the optimized micro reformer and the fixed bed base at the same GHSV = 40,000. (a) The methanol conversion rate of micro reformer; (b) the hydrogen selectivity of micro reformer.

of binder would not be necessary. The pure catalyst, the pure binder, and catalysts with different binder's ratio ranging from 10 to 60 have been tested for surface area and porosity. The experimental result shows that the surface area and porosity gradually increase with increasing of the binder's ratio, as shown in Table 4. This result indicates that the most of revealed surface area for the case of high binder's ratio might be contributed by the high surface

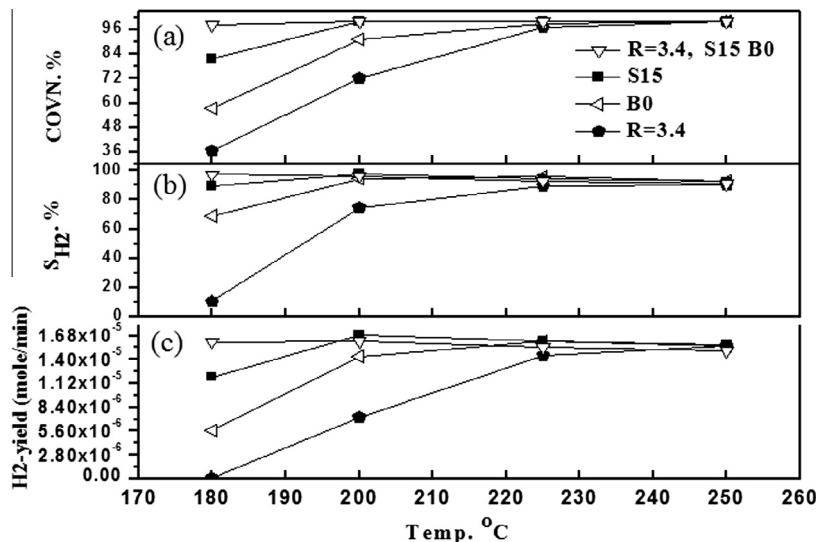


**Fig. 14.** GC analysis results of the optimized micro reformer and the best one for each parameter. (a) The methanol conversion rate of micro reformer; (b) the hydrogen selectivity of micro reformer; (c) the hydrogen yield of micro reformer.

**Table 7**

The activity and throughput of micro methanol reformer.

Reference	Feed rate of methanol (ml/h)	Temp. °C	Catalyst weight (mg)	CONV.%	Throughput, H <sub>2</sub> , L/(h ml mg)	Catalyst bed	Catalyst type	Reaction
[28]	2.14	300	71	98	0.034		CuO/ZnO/Al <sub>2</sub> O <sub>3</sub>	SRM
[29]	2.86	250–290	300	85	0.0075			
[30]	8.57	240–260	300	99	0.012			
[31]	2	270	60	60	0.02			
[26]	1.1	295	135	100	0.019	Packing		
[32]	0.2	270	45	99	0.068			
This study	0.024	180	20	>98	0.074	Slurry	CuO/MnO/ZnO	POM

area of non-catalytic binder which has small-scale particle and porous structure. Hence, the active site of catalyst might be reduced and occupied by the addition of high binder's ratio so that the performance of the micro reformer will be deteriorated. For adding the accommodation ability of the catalyst in micro channels, a minimum value of  $B = 10$  was employed for the rest of the studies with comparable performance to  $B = 0$  but better catalyst adhesion.

### 3.2.3. Solid contents of catalyst solution (S)

To find out the influence of solid catalyst contents to reformer performance, both binder's ratio and channel's aspect ratio were fixed in this study, and the solid content ratio  $S$  was varied from 5% to 15%. The coating process was conducted once instead of 10 times in this study. When  $S$  gradually increases, the viscosity of catalyst solution is increased as well, so as to the reduction of the loading times of catalyst. As the results shown in Fig. 12, where  $S$  was increased from 5% to 15%, the conversion rate of microreformer kept a high performance, close to 100%, and the  $S_{H2}.$ % and  $H_2$ -yield were improved from 88% to 98% and  $1.5 \times 10^{-5}$  to  $1.7 \times 10^{-5}$  (mole/min), respectively, even though the testing temperature was lowered down to 200 °C from 250 °C. Furthermore, at 180 °C, 82% conversion rate, 90% of  $S_{H2}.$ %, and  $1.25 \times 10^{-5}$  (mole/min) hydrogen yield were obtained. On the other hand, the water–gas shift reaction is more obvious than those of other testing parameters in a decrease of hydrogen selectivity and yield rate at almost 100% conversion rate from 200 to 250 °C. Consequently, more hydrogen production can be achieved at lower temperature especially at 200 °C. A high performance, close to 100%, and the  $S_{H2}.$ % and  $H_2$ -yield were improved from 88% to 98% and  $1.5 \times 10^{-5}$  to  $1.7 \times 10^{-5}$  (mole/min), respectively, even though the testing temperature was lowered down to 200 °C from 250 °C. Furthermore, at 180 °C, 82% conversion rate, 90% of  $S_{H2}.$ %, and  $1.25 \times 10^{-5}$  (mole/min) hydrogen yield were obtained. Table 5 from 88 to 98% and  $1.5 \times 10^{-5}$  to  $1.7 \times 10^{-5}$  (mole/min), respectively, even though the testing temperature was lowered down to 200 °C from 250 °C. Furthermore, at 180 °C, 82% conversion rate, 90% of  $S_{H2}.$ %, and  $1.25 \times 10^{-5}$  (mole/min) hydrogen yield were obtained. shows the ICP-MS measurement results of the catalyst amount for different solid contents which is up to 15.1 mg for  $S = 15$ . Fig. 13 shows the SEM images of  $S = 5$  and  $S = 15$ , and the catalyst in Fig. 13(b) is denser than that in Fig. 13(a), attributed to the more viscous catalytic solution at  $S = 15$  to allow more retention of catalyst during drying and calcining process owing that higher the solid content, the more viscose the catalyst solution, which will carry out thicker catalyst layer inside the micro reformer but bear more difficulty on catalyst loading inside microchannel [27]. When combining the results from Figs. 8, 10–12, and Tables 2 and 3, we can summarize that for low-temperature (180 °C) operation with high performance, it is necessary to create a dense catalyst layer coated on the micro channel with a catalyst amount more than 15 mg.

### 3.2.4. Optimization of all the parameters

From the experimental results above, the performance of the micro reformer is much improved especially in the lower operating temperature of 180 °C via adjusting  $R$  from 27.5 to 3.4,  $S$  from 5 to 15, and  $B$  from 60 to 0, as shown in Table 6. For maximize the performance of the micro reformer, an optimized micro reformer was designed and fabricated to include the best conditions of all the investigated parameters for  $R = 3.4$ ,  $S = 15$ , and  $B = 0$  in a testing temperature ranged from 180 to 250 °C. Figs. 14 and 15 show the comparison between the optimized micro reformer, the best reformer of each optimized single parameter, and the traditional fixed bed sample. The result shows the significant and outstanding performance of the optimized micro reformer demonstrating the highest performance at all testing temperatures, with a conversion rate, hydrogen selectivity, and hydrogen yield of nearly 98%, 98% and  $1.6 \times 10^{-5}$  (mole/min), respectively, at 180 °C, which is very close to the performance of fixed bed sample. In a comparison to our micro-reformer and reformers in the literature, Table 7 lists the activity and throughput performance of various methanol reformers with catalysts of Cu/ZnO/Al<sub>2</sub>O<sub>3</sub> or CuO/MnO/ZnO, and reactions in POM or SRM. The results illustrates that the activity of the micro-channel reformers is higher than those in the literature in practice. The micro methanol reformer with  $S = 15$ ,  $R = 3.4$  and  $B = 0$  could produce reformed gas at Hydrogen-throughput of 0.074 (L/(h ml mg)) which is superior to the recent researches. A reformer of this type and design can supply hydrogen to fuel cells that can produce approximately 2.23 J/min with 80%  $H_2$  utilization and 60% fuel cell efficiency at 2 ml/min of reactant gas feeding rate.

## 4. Conclusions

A micro-methanol reformer with finger-shaped channel which can be operated in low temperature with high-conversion efficiency and high hydrogen throughput have been successful designed and demonstrated in this study. The performance of the micro-channel reformer is influenced by the reactive area for methanol reforming and the amount of catalyst contained in the micro channel. Therefore, a large reactive area and amount of the catalyst can be realized via applying centrifugal coating process, optimizing the channel's aspect ratio, increasing the solid contents, and decreasing the binder's ratio in the catalytic slurries. 98% of methanol conversion rate, 98% of hydrogen selectivity,  $1.6 \times 10^{-5}$  (mole/min) of hydrogen yield, and 0.074 of hydrogen throughput of the an optimized micro reformer can be obtained at 180 °C under a testing condition when  $R = 3.4$ ,  $S = 15$  and  $B = 0$ . This micro reformer can supply hydrogen to fuel cells that can produce approximately 2.23 J/min with 80%  $H_2$  utilization and 60% fuel cell efficiency at 2 sccm of reactant gas feed rate.

## Acknowledgment

The authors would like to thank National Science Council of Taiwan for the financial support (NSC101-3113-E-007-001).

## References

- [1] Kawamura Y, Ogura N, Yamamoto T, Igarashi A. A miniaturized methanol reformer with Si-based microreactor for a small PEMFC. *J Chem Eng Sci* 2006;61:1092–101.
- [2] Holladay JD, Wainright J, Jones EO, Gano SR. Power generation using a mesoscale fuel cell integrated with a microscale fuel processor. *J Power Sources* 2004;130:111–8.
- [3] de Wild PJ, Verhaak MJFM. Catalytic production of hydrogen from methanol. *Catal Today* 2000;60:3–10.
- [4] Alejo L, Lago R, Pena MA, Fierro JLG. Partial oxidation of methanol to produce hydrogen over Cu/Zn-based catalysts. *Appl Catal A* 1997;162:281–97.
- [5] Cheng WH, Kung HH. Methanol Production and Use, 1994. p. 1.
- [6] Holladay JD, Jones EO, Dagle RA, Xia GG, Cao C, Wang Y. High efficiency and low carbon monoxide micro-scale methanol processors. *J Power Sources* 2004;131:69–72.
- [7] Terazaki T, Nomura M, Takeyama K, Nakamura O, Yamamoto T. Development of multi-layered microreactor with methanol reformer for small PEMFC. *J Power Sources* 2005;145:691–6.
- [8] Turco M, Bagnasco G, Costantino U, Marmottini F, Montanari T, Ramis G, et al. Production of hydrogen from oxidative steam reforming of methanol II. Catalytic activity and reaction mechanism on Cu/ZnO/Al2O3 hydrotalcite-derived catalysts. *J Catal* 2004;228:56–65.
- [9] Kwon OJ, Yoon DH, Kim JJ. Silicon-based miniaturized reformer with methanol catalytic burner. *Chem Eng J* 2008;140:466–72.
- [10] Kim T, Kwon S. Catalyst preparation for fabrication of a MEMS fuel reformer. *Chem Eng J* 2006;123:93–102.
- [11] Park GG, Seo DJ, Park SH, Yoon YG, Kim CS, Yoon WL. Development of microchannel methanol steam reformer. *Chem Eng J* 2004;101:87–92.
- [12] Zeng D, Pan M, Wang L, Tang Y. Fabrication and characteristics of cube-post microreactors for methanol steam reforming. *Appl Energy* 2013;91:208–13.
- [13] Amphlett JC, Creber KAM, Davis JM, Mann RF, Peppley BA, Stokes DM. Hydrogen production by steam reforming of methanol for polymer electrolyte fuel cells. *Int. J Hydrogen Energy* 1994;19:131–7.
- [14] Raboij LPLM. Modeling of a variable-flow methanol reformer for a polymer electrolyte fuel cell, hr. *J. Hydrogen Energy* 1995;20:845–8.
- [15] Acrela GJK, Frosta JC, Hards GA, Pottera RJ, Ralph TR, Thompsett D, et al. Electrocatalysts for fuel cells. *Catal Today* 1997;38:393–400.
- [16] Hsieh SS, Yang SH, Kuo JK, Huang CF, Tsai HH. Study of operational parameters on the performance of micro PEMFCs with different flow fields. *Energy Convers Manage* 2006;47:1868–78.
- [17] Ananthakumar S, Raja V, Warrier KGK. Effect of nanoparticulate boehmite sol as a dispersant for slurry compaction of alumina ceramics. *Mater Lett* 2000;43:174–9.
- [18] Hwang SM, Kwon OJ, Kim JJ. Method of catalyst coating in micro-reactors for methanol steam reforming. *Appl Catal A* 2007;316:83–9.
- [19] Kwon S, Messing GL. Constrained densification in boehmite alumina mixtures for the fabrication of porous alumina ceramics. *J Mater Sci* 1998;15:913–21.
- [20] Pattekar AV, Kothare MV. A microreactor for hydrogen production in micro fuel cell applications. *J Microelectromech Syst* 2004;13:7–18.
- [21] Pfeifer P, Scjibert K, Liauw MA, Emig G. PdZn catalysts prepared by washcoating microstructured reactors. *Appl Catal A* 2004;270:165–75.
- [22] Haas-Santo K, Fichtner M, Schubert K. Preparation of microstructure compatible porous supports by sol-gel synthesis for catalyst coatings. *Appl Catal A* 2001;220:79–92.
- [23] Huang YJ, Ng KL, Huang HY. The effect of gold on the copper-zinc oxides catalyst during the partial oxidation of methanol reaction. *Int J Hydrogen Energy* 2011;36:15203–11.
- [24] Huang CC, Huang YJ, Wang HS, Tseng FG, Su YC. A well-dispersed catalyst on porous silicon micro-reformer for enhancing adhesion in the catalyst-coating process. *Int J Hydrogen Energy* 2014;39:7753–64.
- [25] Lee KY, Shen CC, Huang\* YJ. Enhancement of partial oxidation of methanol reaction over CuZn catalyst by Mn promoter. *Ind Eng Chem Res* 2014;53(32):12622–30.
- [26] Lim MS, Kim MR, Noh J, Woo SI. A plate-type reactor coated with zirconia-sol and catalyst mixture for methanol steam-reforming. *J Power Sources* 2005;140:66–71.
- [27] Bravo J, Karim A, Conant T, Lopez Gp, Datye A. Wall coating of a CuO/Zn/Al2O3 methanol steam reforming catalyst for micro-channel reformers. *Chem Eng J* 2004;101:113–21.
- [28] Leu CH, Chen CC, King SC, Huang JM, Tzeng SS, Chang WC. Influence of CuO/ZnO/Al2O3 wash-coating slurries on the steam reforming reaction of methanol. *Int J. Hydrogen Energy* 2011;36:12231–7.
- [29] Park GG, Yim SD, Yoon YG, Kim CS, Seo DJ, Eguchi K. Hydrogen production with integrated microchannel fuel processor using methanol for portable fuel cell systems. *Catal Today* 2005;110:108–13.
- [30] Park GG, Yim SD, Yoon YG, Lee WY, Kim CS, Seo DJ. Hydrogen production with integrated microchannel fuel processor for portable fuel cell systems. *J Power Sources* 2005;145:702–6.
- [31] Chein RY, Chen YC, Lin YS, Chung JN. Hydrogen production using integrated methanol-steam reforming reactor with various reformer designs for PEM fuel cells. *Int J Energy Res* 2012;36:466–76.
- [32] Kundu A, Ahh JE, Park SS, Shul YG, Han HS. Process intensification by micro-channel reactor for steam reforming of methanol. *Chem Eng J* 2008;135:113–9.